Powder Technology 480 (2026) 122661

Contents lists available at ScienceDirect

Powder Technology

journal homepage: www.journals.elsevier.com/powder-technology

Thermal effects in mechanically induced phase transformations in Co powders

Marta Cappai [a], Maria Carta [a,b], Giorgio Pia [a], Francesco Delogu [a,b,*]

[a] Department of Mechanical, Chemical and Materials Engineering, University of Cagliari, via Marengo 2, 09123 Cagliari, Italy
[b] CSGI Research Unit, University of Cagliari, via Marengo 2, 09123 Cagliari, Italy

HIGHLIGHTS

- We used ball milling to induce the hcp-to-fcc phase transformation in Co powders.
- We studied how temperature and impact energy affect the transformation kinetics.
- We developed a kinetic model to properly identify meaningful rate constants.
- Higher temperatures result in reduced rate constants and higher activation energies.
- We explain the observations with a competition between defect generation-recovery.

GRAPHICAL ABSTRACT

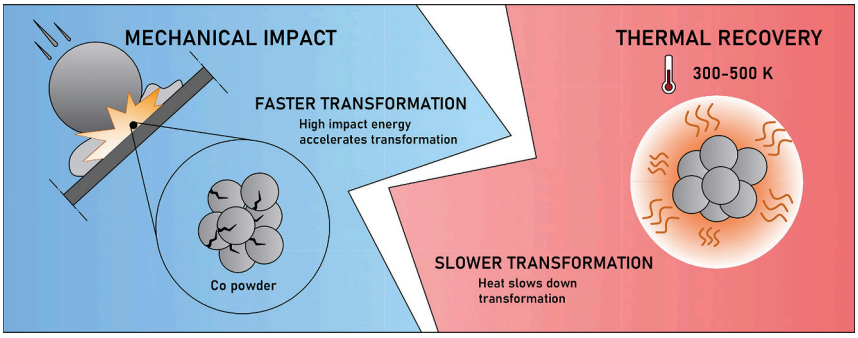

ARTICLE INFO

Keywords:
Co powders
ball milling
mechanical processing
phase transformation
temperature

ABSTRACT

The mechanical processing of Co powders by ball milling is known to induce a phase transformation between the two allotropic forms of Co with hexagonal close-packed and face-centred cubic crystalline structures. The same phase transformation can be also activated and driven by gradual heating or isothermal annealing. For this reason, it is reasonable to expect that temperature plays an important role also during the mechanical processing. In this work, we investigate exactly how temperature affects the phase transformation behaviour by ball milling Co powders at different milling frequencies and temperatures between 300 K and 500 K. Unexpectedly, we find that, regardless of the milling frequency, any temperature increases results in a decrease of the phase transformation rate. We tentatively explain the experimental findings by considering thermally activated recovery processes.

1. Introduction

Mechanochemistry does not cease to show an impressive vitality for about 60 years [1–3]. Starting from the end of 1960s, it has literally changed the face of powder metallurgy, first, and then, materials science [4–7]. Now, after one moment of flux approximately at the end of 2010s, mechanochemistry has gained ground in inorganic and organic synthesis due to its promise of enhancing the sustainability of chemical industry through the reduction, or even the elimination, of solvent in production processes [8–12]. The results obtained in this respect are

* Corresponding author at: Department of Mechanical, Chemical and Materials Engineering, University of Cagliari, via Marengo 2, 09123 Cagliari, Italy.
E-mail address: francesco.delogu@unica.it (F. Delogu).

https://doi.org/10.1016/j.powtec.2026.122661
Received 2 March 2026; Received in revised form 19 April 2026; Accepted 5 May 2026
Available online 8 May 2026

currently driving mechanochemical methods to an important role in the panorama of technological innovation [13–15].

The tangible prospect of application and the long tradition of research in mechanochemistry clash with the unsatisfactory level of understanding of its fundamentals achieved so far [16–18]. The reason for this situation definitely lies in the inherent complexity of mechanochemical transformations [6,19–23].

The mechanical processing is intrinsically discontinuous and non-uniform [17,24]. The solids in powder form experience deformation at high strain rates and are driven far from thermodynamic equilibrium [25,26]. The generation of structural defects is partially counterbalanced by their annihilation due to simultaneous relaxation and recovery processes that compete with one another [23,27]. Thus, the final products of mechanically induced transformations are the result of mechanisms that involve several time and length scales [22,24,25,28–32].

Further difficulties arise from the lack of information on the processing conditions [17,19,25,28,30–32]. In most cases, only the experimental variables that govern the operation of the apparatuses used to process the substances are specified and no attempt is made to gain insight into the conditions really experienced by the powder materials at the scale of individual particles and below [19,24–26,28,30,32].

Ball milling (BM) represents a typical example in this regard. Reporting the milling frequency, the reactor size and shape, the number of balls and their size and shape, the amount of material inside the reactor is useful, but it cannot tell the whole story. BM conditions are made of suitably evaluated impact frequencies, impact energies, impact angles, impact durations and still other quantities related to the dynamic compaction processes undergone by powders compressed during impacts. And even with these quantities we are far from seeing the whole picture.

Under these circumstances, even the simplest questions can remain unanswered. One of these concerns temperature, which is quite surprising in the light of the central role it normally plays in chemistry. We do not know yet how temperature can affect mechanochemical transformations. The reasons are many. First of all, BM is typically performed at room temperature, so that we have only a few data coming from experiments performed at other nominal temperatures. Early experiments on brittle materials such as Ge-Si and Mn-Bi showed that cryogenic cooling is sufficient to suppress mechanical alloying entirely, indicating that thermally activated processes cannot be neglected [33]. Systematic studies of the Ag-Cu metallic system over the range 85–473 K showed that higher temperatures promote decomposition of the mechanically induced metastable phases [34], while milling of iron powders under reactive atmospheres demonstrated that lower temperatures favour the formation of metastable nitrogen-rich phases [35]. More recently, high-temperature BM of Ti-based metallic powders was shown to promote phase transformations and the formation of fcc-rich regions [36,37], while reactive BM of Mg-Ni systems demonstrated that higher temperatures accelerate hydride formation kinetics [38]. Most recently, BM of Co powders at 750 K was shown to intensify the hcp-to-fcc transformation relative to dynamic annealing at the same temperature, demonstrating that mechanical impacts contribute to the transformation kinetics independently of the thermal driving force [39]. Notwithstanding this recent progress, most of the available datasets were not collected changing systematically the temperature while characterizing properly the BM conditions. Finally, the chemical systems investigated at different temperatures are just a few and very different from one another. As a consequence, experimental evidence is contradictory overall. Sometimes higher temperatures are beneficial, sometimes they negatively affect the transformation rate or even change the final product [4].

In this work, we address the open question regarding the role of temperature in BM by studying the phase transformation behaviour of Co powders. This choice is motivated by the fact that Co bulk systems can undergo a martensitic phase transition at ambient pressure between two allotropic crystalline structures [40–45]. From room temperature to about 700 K, the hexagonal close-packed (hcp) phase is the stable phase. Above this temperature, the hcp phase transforms into a face-centred cubic (fcc) phase with a latent heat equal to about 400 J mol^{-1} [40–45].BM can also induce the hcp-to-fcc transformation, which occurs at rates that scale linearly with the impact energy [46–49].

Here, we present the results of an experimental investigation based on the systematic change of the impact energy and the temperature at which BM is performed. The results clearly show that, regardless of the impact energy characterizing the intensity of BM, temperature affects the hcp-to-fcc phase transformation rate. In particular, the phase transformation rate surprisingly decreases with temperature. We tentatively explain the experimental findings by considering the effects of relaxation and recovery process within the framework of a kinetic model.

2. Materials and methods

BM experiments were performed using high-purity commercial Co powders purchased from Sigma Aldrich. The powders were sieved to select a particle size below 10 μm and annealed for 24 h at 473.15 K in an oven under a flux of Ar and H_2 to eliminate humidity and surface oxides. Then, they were stored in a glove box under Ar atmosphere with H_2O and O_2 contents below 2 ppm. Annealed and processed powders were invariably handled inside the glove box, which avoided any exposure to ambient atmosphere.

With no a priori information available on the extent of possible thermal effects on the hcp-to-fcc phase transformation induced by BM, we had no alternative than performing a significant number of preliminary experiments to set up the experimental apparatus and fine-tune the BM conditions.

BM experiments were carried out using a Spex Mixer/Mill 8000 equipped with a variable speed electric motor. This ball mill imparts three-dimensional oscillations to the reactor, allowing an optimal stirring of loose powders. By changing the rotational speed of the motor, we changed the frequency of the reactor motion between 14 Hz and 22 Hz.

We used a hardened-steel cylindrical reactor with flat bases and a total volume of about 60 cm^3. Inside it, we placed a single stainless-steel ball of 12 g and a mass of Co powder equal to 10 g. The choice of using a single ball and 10 g of Co powder was strictly related to the need of characterizing and controlling accurately the BM conditions. In fact, we are able to detect all the ball impacts on the reactor bases and side wall as far as a single ball is used [27,50,51].

To this aim, we attached a piezoelectric sensor to one of the reactor ends and recorded the signals generated by the vibrations originated in the reactor body by each impact. The piezoelectric signals were suitably analyzed and a time series was obtained consisting of the instants at which impacts are detected [27,50,52].

Such time series were compared with the corresponding ones obtained by reconstructing the ball motion inside the moving reactor via numerical simulation [53,54]. In this case, not only we had a time series of impacts, but also fine details associated with individual impacts such as impact velocity and angle. The vial motion was described analytically as a combination of synchronous roto-translations in the inertial reference frame. Between consecutive impacts, the equations of motion reduce to uniform rectilinear motion, gravity being negligible compared to the accelerations imparted by the vial [53–55]. The ball position was updated step by step using the Verlet algorithm with a time step equal to 10^{-5}, chosen to match the collision duration estimated from Hertzian contact theory. Impacts were modelled as instantaneous events: the component of the relative impact velocity perpendicular to the impacted surface was reversed and scaled by a coefficient of restitution, e, that measures the degree of impact elasticity [53–55]. The simulation provided the time series of impacts and the associated impact velocities, angles, and energies.

Taking advantage of long time series, we sought the best

correspondence between experimental and numerical data by changing the impact elasticity in calculations. In particular, we compared the statistical distributions of the time interval between consecutive impacts. Once the experimental and numerical distributions overlapped to a satisfactory extent, we associated the impact velocity, angle and elasticity obtained from simulations with the real processing conditions [23,51,54,56,57].

Impact elasticity is related to the mass of powder inside the reactor and its properties, flowability in particular. For loose powders such as Co ones, we observed a proportionality between the mass of powder and the coefficient of restitution estimated by numerical simulation, which provides an average measure of the impact elasticity degree. In this work, we did not change the total amount of powder inside the reactor, keeping it equal to 10 g in all the BM experiments. Nevertheless, our analyses indicate a small change of the coefficient of restitution with the milling frequency, which we ascribe to the corresponding change of the average impact velocity.

The combined experimental-numerical methodology adopted in this work has been progressively developed in a series of previous studies. The methodology encompasses the piezoelectric detection of ball-reactor impacts [27,50,52], the numerical reconstruction of the three-dimensional ball trajectory inside the Spex Mixer/Mill 8000 reactor [53], and the nonlinear dynamics analysis of the chaotic character of the ball motion and its dependence on the coefficient of restitution [54,55,58], which underpins the statistical comparison of experimental and numerical inter-impact time distributions used to estimate the effective restitution coefficient. The application of this combined approach to the quantitative study of mechanically induced phase transformation kinetics is documented in earlier work [23,56,57]. This framework allowed us to characterize the milling dynamics to a remarkable extent. Accordingly, it also enabled us to control the BM conditions by selecting the desired impact energy. The methodology provided the basis for a reliable kinetic investigation of the hcp-to-fcc phase transformation undergone by Co powders and the detection of the thermal effects accompanying the increase of the reactor temperatures.

To change and control temperature, the reactor was equipped with a handcrafted heating element consisting of an electrically powered ceramic ring that can reach temperatures as high as 750 K and a thermocouple. The heating element was fixed around the cylindrical reactor body, while the thermocouple was attached to one of the reactor ends. Heating element and thermocouple were connected with a computer that allowed to control the average reactor temperature and keep it constant at the desired value. A schematic description of the experimental set-up is shown in Fig. 1.

The cylindrical reactor body is surrounded by the ring heating element. A piezoelectric sensor is fixed to one of the reactor ends and a thermocouple is attached to the opposite one. Thin cylinders in refractory material are used to isolate the reactor from the clamp assembly. In this way, the heat generated by the heating element remains substantially confined to the reactor and does not propagate to the gear of the ball mill, which would be potentially harmful. In any case, we performed the BM experiments at temperatures between 300 K and 500 K to avoid damaging the gear of the ball mill.

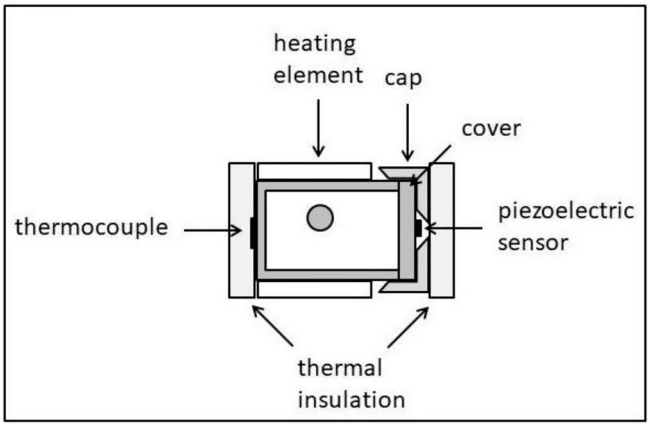

Fig. 1. The reactor set-up utilized in BM experiments. The schematic representation is not to scale.

To assess the temperature homogeneity inside the reactor, we performed dedicated measurements by placing thermocouples at different positions on the reactor surface (both ends and mid-section) during heating without milling. The temperature differences across the reactor body were found to be within ±5 K at steady state for all the temperatures investigated (300–500 K). This is consistent with the short characteristic thermal diffusion time across the reactor wall, estimated as $L^2/\alpha \approx 6$ s, where $L \approx 5$ mm is the wall thickness and $\alpha \approx 4$ mm^2 s^{-1} is the thermal diffusivity of steel. This time is much shorter than the duration of our BM experiments. The high thermal conductivity of the steel reactor body and the small reactor volume, combined with the three-dimensional motion of the reactor and the continuous stirring of the powder charge during milling, further promote temperature equalization inside the reactor. On these grounds, we consider the temperature homogeneity adequate for the purposes of our investigation.

A FEI Quanta 200 scanning electron microscope was also used to monitor the change of particle size and morphology during the mechanical processing.

We carried out the kinetic investigation by analyzing the Co powders by X-ray diffraction (XRD) using a Rigaku D/Max diffractometer equipped with Cu Kα radiation. XRD patterns were collected on Co powders sampled from the reactor after selecting time periods of mechanical processing. To this aim, BM was interrupted and the reactor rapidly cooled using powerful jets of cold air. Then, the reactor was opened inside the glove box under Ar atmosphere with oxygen and humidity contents below 2 ppm. The sampled Co powders were cold-compacted in disk-shaped specimens and XRD patterns were collected over a range of scattering angle, 2θ, from 20° to 120°, in steps of 0.05° with acquisition time of 20 s per angle. Cold compaction ensures a statistically random particle orientation, which is essential for reliable Rietveld refinement. The quasi-static, low-pressure loading involved does not drive the hcp-to-fcc transformation.

In preliminary experiments, we ascertained that the relative amounts of hcp and fcc phases in Co powders do not change during the reactor cooling process. This was done by preparing mixtures with different relative contents of hcp and fcc phases, and subjecting them to heating and cooling cycles. A total of six heating and cooling cycles were performed. We found no significant difference in the fractions of hcp and fcc phases before and after the heating and cooling cycles. Therefore, the fractions that we estimated by the Rietveld analysis of XRD patterns after the Co powder sampling can be considered reliable estimates.

We used the measured fractions of hcp and fcc phases to build kinetic curves. In such curves, any given experimental point is the average of at least five different measurements. Whenever necessary, BM experiments were repeated up to ten times. Error bars for individual points correspond to the standard deviation of the estimates obtained in different measurements.

We did not observe any significant increase of Fe impurities due to contamination from reactor wear. The Fe content, estimated by X-ray fluorescence, keeps approximately constant at about 8 ppm. Similarly, there was no significant oxidation of Co powders. Thus, it can be reasonably inferred that the observed hcp-to-fcc phase transformation behaviour of Co powders during the BM process cannot be ascribed to contamination effects.

3. BM conditions

The combined use of experiments and calculations allows gaining

significant insight into the ball dynamics underlying the processing conditions that Co powders experience during the BM experiments. Piezoelectric transducers readily detect the impacts between ball and reactor, thus providing information on the ball motion inside the moving reactor in the presence of 10 g of Co powder. A short excerpt from a typical time series of impacts is shown in Fig. 2a.

Raw data obtained from the piezoelectric sensors have already filtered with a classical method based on fast Fourier transform. The resulting signals appear well defined, almost equally spaced from one another. Numerical simulations allow obtaining a similar time series. Part of it is also shown in Fig. 2a, which allows appreciating the almost perfect correspondence between experimental and numerical datasets. Estimating the impact frequency, N, is straightforward from both experimental and numerical impact sequences.

A suitable choice of the coefficient of restitution, e, which measures the impact elasticity, invariably allows to obtain from numerical simulations exactly the same N value measured from experimental time series. In addition, it is also possible to find a very good correspondence between the statistical distribution $p(\Delta t)$ of the time intervals between consecutive impacts obtained experimentally and numerically. A representative example is shown in Fig. 2b.

Once we have obtained the best correspondence between experiments and simulations, we can associate to experiments the estimates of impact velocity, v, and energy, E, obtained from calculations. These are the quantities of interest for the kinetic analysis of the hcp-to-fcc phase transformation.

Based on the correspondence of experimental and numerical datasets obtained under all the different BM conditions explored, we have been able to characterize the BM conditions using the quantities reported in Table 1.

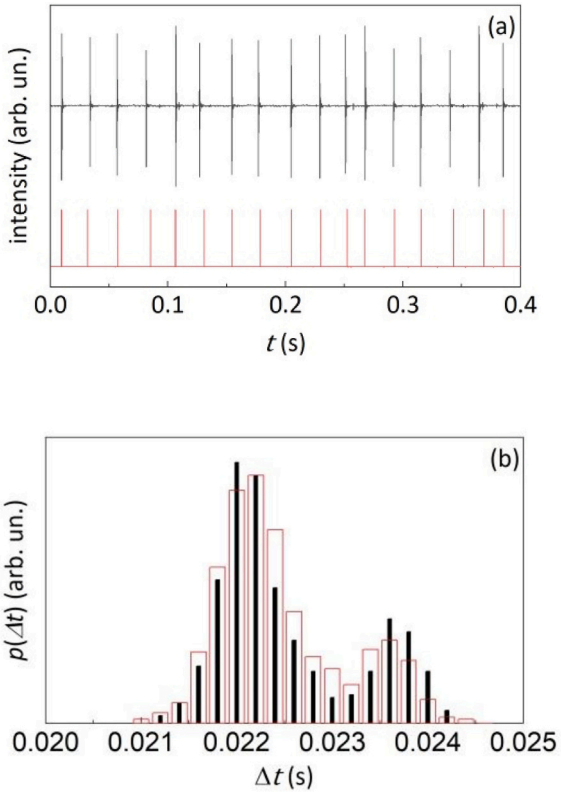

Fig. 2. (a) Typical sequences of impacts from experiments (black line) and numerical simulation (red line). (b) Statistical distributions $p(\Delta t)$ of the time intervals between consecutive impacts obtained experimentally (black columns) and numerically (red columns). Data refer to BM experiments performed at 22 Hz and 300 K. (For interpretation of the references to colour in this figure legend, the reader is referred to the web version of this article.)

Table 1
Milling frequency, f (Hz), impact frequency, N (Hz), average impact velocity, v ($m{\cdot}s^{-1}$), and coefficient of restitution, e, characterizing the BM experiments performed. All parameters were determined at room temperature (approximately 300 K).

f	N	v	e
14	28.2	3.94	0.09
16	32.3	4.50	0.10
18	35.9	5.07	0.13
20	40.1	5.64	0.12
22	44.4	5.88	0.16

Data in Table 1 clearly indicate that the impact frequency N is proportional to the milling frequency f. In particular, N is approximately twice f in all the five cases investigated. This strongly suggests that the ball undergoes a regular displacement between the opposite bases, which involves two impacts per reactor cycle [27,50,52,55,58]. The ball trajectories that are reconstructed in numerical simulations confirm the inference based on the simple experimental evidence [53,54]. The ball moves periodically between the two reactor bases with only minor interactions with the reactor side wall. It is worth noting that these occasional contacts introduce minor perturbations in the impact timing that account for the small but systematic deviation of the ratio N/v from the exact value of 2. Accordingly, we can restrict our analysis to the impacts that occur on the reactor bases, which determine the overall impact frequency N and the average impact velocity v. In this regard, it is worth noting that the contacts between ball and reactor side wall are definitely less energetic than those involving the reactor bases. Indeed, the average impact velocity on the reactor side wall is on the order of 1 $m{\cdot}s^{-1}$ [53,54]. We expect that the main contribution to the hcp-to-fcc phase transformation comes from impacts at higher velocity.

Numerical simulations indicate an increase of the impact velocity v with the milling frequency f. As shown in Fig. 3, the increase is approximately linear and it also affects the impact elasticity. In fact, the coefficient of restitution e increases with the impact velocity v. The faster the ball moves, the higher the impact elasticity degree, which is expected based on classical notions of contact mechanics.

We can add that the 10 g of Co powders present inside the reactor have a significant effect on the impact elasticity. The coefficient of restitution, e, for a stainless steel ball impacting on a stainless steel flat surface takes values around 0.5, which means that half of the ball kinetic energy is dissipated as heat at the impact. The e values that we eventually obtain from the comparison of experimental and numerical datasets are much smaller. This means that impacts are characterized by significant inelasticity due to the fact that a certain amount of powder is compressed between the impacting surfaces of ball and reactor. Due to the work done in compressing the powder, every time the ball impacts the reactor bases, it loses almost completely its kinetic energy.

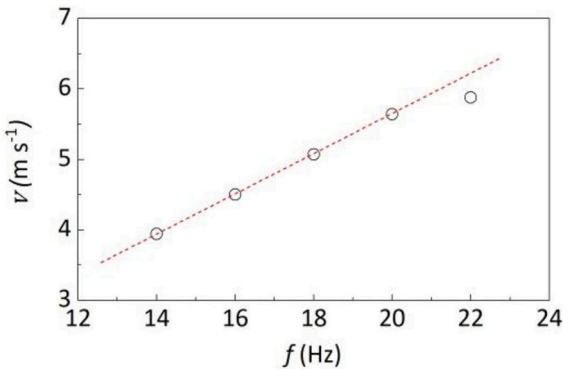

Fig. 3. The average impact velocity, v, as a function of the milling frequency, f. The plotted line is a guide to the eyes.

4. Experimental evidence

Mechanical processing by BM determines a progressive reduction of Co particle size, as shown by the representative SEM micrographs reported in Fig. 4. Fig. 4a gives information on particle size and morphology before mechanical processing. Fig. 4b shows that the repeated deformation undergone by powder particles during impacts gradually hardens the metal and reduces its particle size.

The sequences of experimental XRD patterns reported in Fig. 5 for milling temperatures of 300 K (Fig. 5a), 400 K (Fig. 5b), and 500 K (Fig. 5c) reveals the gradual broadening of crystalline reflections and the progressive growth of new broad peaks. Broadening can be ascribed to the refinement of grain size and the disordering of the crystalline lattice, which leads to the formation of a nanostructure. This is accompanied by the gradual transition from the initial hcp phase to the final fcc one, which becomes evident from the appearance of new peaks.

Crystalline reflections allow monitoring the hcp-to-fcc phase transformation to a very good extent. Although the peaks of the hcp and fcc phases partially overlap, the phase evolution can be followed to a remarkable extent. The Rietveld analysis provides satisfactory results. The best fitted Rietveld profile overlaps almost perfectly the experimental XRD patterns. Across all experimental conditions investigated, the Rietveld refinements consistently yield reliability indicators in the range $R_p \approx 10\%$, $R_{wp} \approx 9\%$, and $\chi 2 \approx 1.4$, confirming the quality of the fits. A representative example is shown in Fig. 6, where the experimental XRD pattern collected after 244 min of BM at 400 K is reported together with the best fitted Rietveld profile and the corresponding difference curve in the 2θ range from 30° to 70°. The formation of a nanostructured hcp phase is faster than the hcp-to-fcc transition. Therefore, it is reasonable to say that the formation of the fcc phase occurs at the expenses of the nanostructured Co hcp phase. The Rietveld analysis suggests that the average grain size of the nanostructured hcp phase is approximately equal to 35 nm, while its average lattice strain ranges between 0.01 and 0.03. The fcc phase has average grain size of about 30 nm and average lattice strain around 0.04.

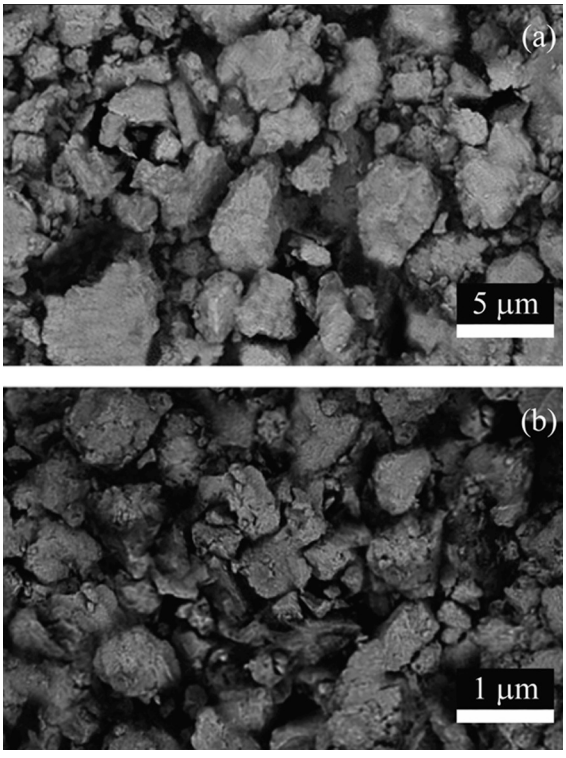

Fig. 4. SEM micrographs of Co powders (a) before and (b) after 50 min of BM. After 50 min of BM, a clear reduction in particle size is observed.

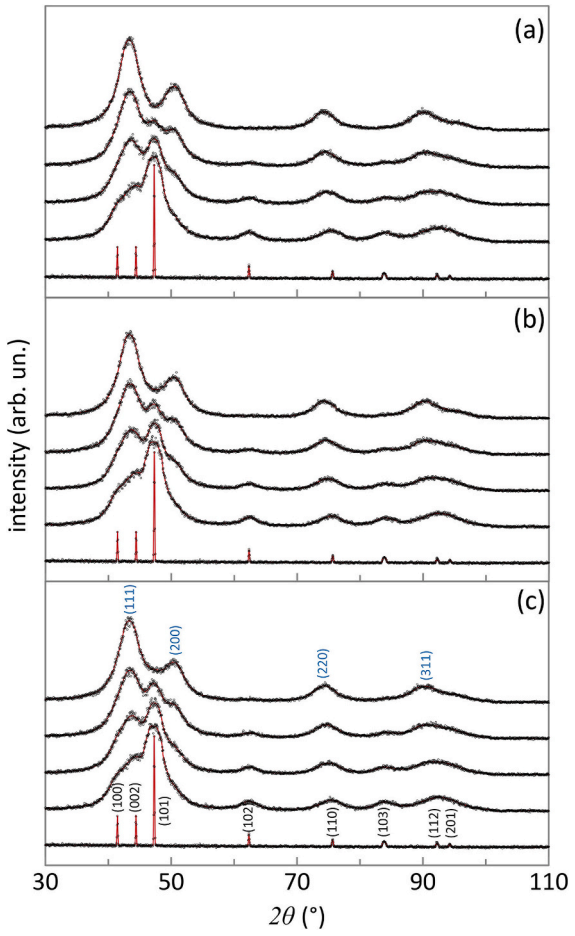

Fig. 5. XRD patterns describing the gradual hcp-to-fcc phase transformation undergone by Co powders during mechanical processing by BM. Scattered intensity is plotted as a function of the scattering angle 2θ. Data refer to BM experiments performed at 20 Hz and (a) 300 K, (b) 400 K, and (c) 500 K. In each series, XRD patterns refer to powders sampled after 0, 50, 120, 244, and 520 min of BM, from bottom to top. The Miller indices (*hkl*) of the main reflections of the hcp and fcc phases of Co are indicated in (c) and apply to all patterns.

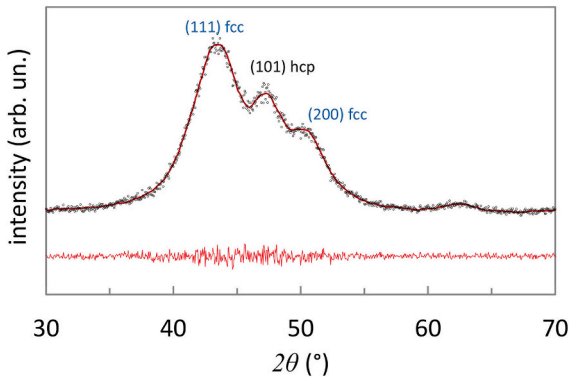

Fig. 6. A detail of the XRD pattern of Co powders sampled after 244 min of BM at 400 K. Experimental data (black dots) and the overall Rietveld profile (red curve) are shown. The difference between the two datasets is also shown (bottom, red line). (For interpretation of the references to colour in this figure legend, the reader is referred to the web version of this article.)

The considerations made so far for the XRD patterns shown in Fig. 5 hold true for all the experimental datasets. Regardless of the experimental BM conditions utilized, Co powders display the same structural

and microstructural behaviour, although BM conditions affect the rate at which structure and microstructure change.

The Rietveld analyses allowed reliably estimating the fractions of hcp and fcc phases and, then, reconstructing the kinetic curves describing the hcp-to-fcc phase transformation. A representative example is shown in Fig. 7a, where the fraction of fcc phase, $\chi_{fcc}(m)$, is plotted as a function of the total number of impacts, m. This quantity was obtained by simply multiplying the impact frequency, N, by the time of mechanical processing experienced by the powders. The $\chi_{fcc}(m)$ values increase monotonically at a rate that becomes slower and slower, which means that $\chi_{fcc}(m)$ approaches 1 asymptotically.

The same data are shown in a semi-logarithmic plot in Fig. 7b. Data arrange according to an almost perfectly linear trend, which indicates that the kinetic curve has definite exponential character.

All the different kinetic curves obtained under different BM conditions exhibit the same exponential character. The kinetics of the hcp-to-fcc phase transformation induced by BM is described by exponential curves. This makes particularly simple to evaluate the phase transformation rate, $r(E;T_{amb})$, which corresponds to the slope of the linear semi-logarithmic plots.

We performed BM experiments in which the milling frequency, f, and the average reactor temperature, T_{amb}, were changed respectively between 14 Hz and 22 Hz, and between 300 K and 500 K. The $r(E;T_{amb})$ datasets obtained are shown in Fig. 6a and b as a function of impact energy, E, and reactor temperature, T_{amb}, respectively.

The data plotted in Fig. 8a point out that impact energy has a profound effect on the hcp-to-fcc phase transformation rate. To a first approximation, $r(E;T_{amb})$ increases linearly with E in all cases. However, linearity seems to worsen for the BM experiments performed at the highest temperatures.

The effects of temperature T_{amb} on the phase transformation rate

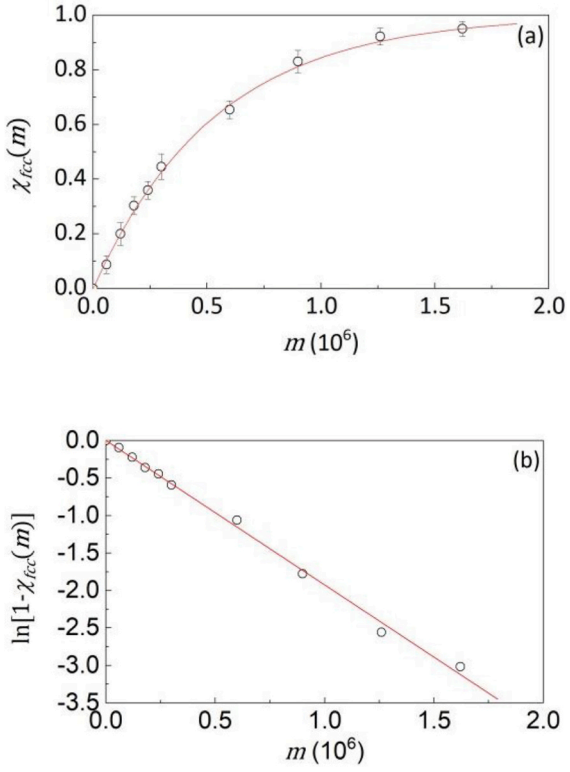

Fig. 7. (a) The fraction of fcc phase, $\chi_{fcc}(m)$, and (b) the logarithm of $1-\chi_{fcc}(m)$, $\ln\left[1-\chi_{fcc}(m)\right]$, as a function of the total number of impacts, m. Data refers to Co powders that underwent BM at 20 Hz and 400 K. Best-fitted curve and line are shown.

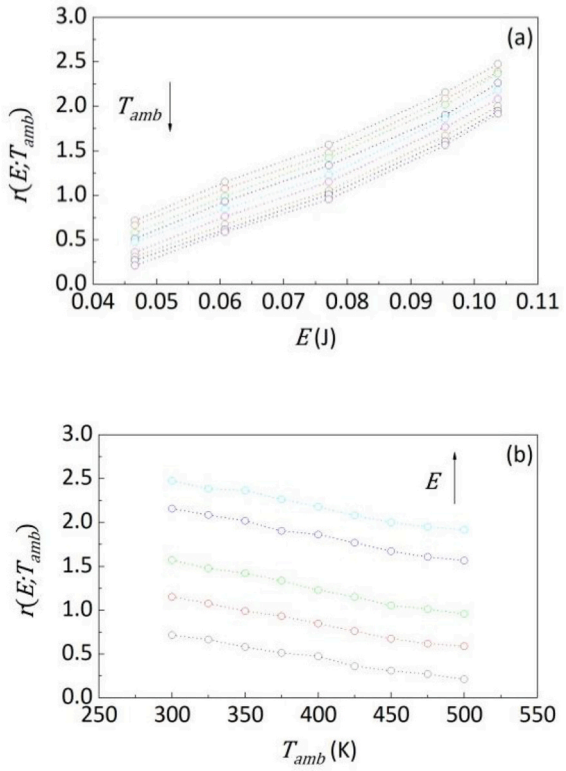

Fig. 8. The hcp-to-fcc phase transformation rate, $r(E;T_{amb})$, as a function of (a) impact energy, E, and (b) reactor temperature, T_{amb}. The arrows indicate the direction in which temperature and impact energy increase respectively in panel (a) and (b).

$r(E;T_{amb})$ are more evident in Fig. 8b. Being the impact energy the same, the increase of temperature induces a decrease of $r(E;T_{amb})$. Such decrease appears quite linear, particularly for the BM experiments carried out at the lowest temperatures. This trend is also visually apparent from the comparison of the XRD sequences shown in Figs. 5a-c.

We best fitted the linear arrangements of data in Fig. 8a and b with lines. We find that the slope of best fitted lines in Fig. 8a, ρ_E, remains approximately constant regardless of the temperature T_{amb}, its average value being equal to about $29.7 \times 10^{-5}\,J^{-1}$. The slope of the linear plots in Fig. 8b is negative and also approximately constant, its absolute value being equal to about $2.92 \times 10^{-3}\,K^{-1}$; such quantity is hereafter denoted as ρ_T.

The $r(E;T_{amb})$ datasets obtained at T_{amb} values equal to 300 K and 500 K are re-plotted in Fig. 9 with the purpose of pointing out another aspect of the linear dependence of $r(E;T_{amb})$ on E. Specifically, it can be

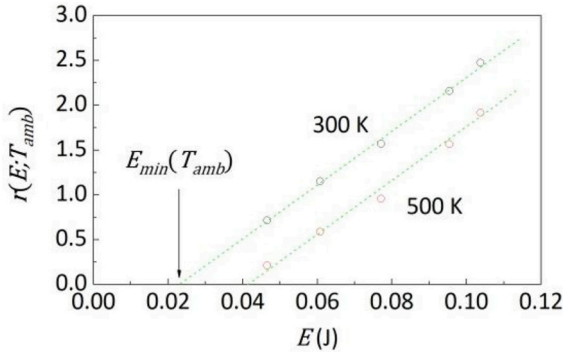

Fig. 9. Datasets of the hcp-to-fcc phase transformation rate, $r(E;T_{amb})$, collected at temperatures T_{amb} of 300 K and 500 K as a function of impact energy, E. Best-fitted lines are shown.

seen that the best fitted lines cross the abscissa axis at a finite, positive value of impact energy that varies with the temperature T_{amb}. Such value, hereafter denoted as $E_{min}(T_{amb})$, can be regarded as the minimum impact energy that must be delivered to Co powders to induce the phase transformation. This is actually confirmed by BM experiments performed at 300 K using a single stainless-steel ball of 4 g and a milling frequency of 14 Hz. No phase transformation was detected after 48 h of uninterrupted BM.

Overall, the linear dependence of the phase transformation rate on impact energy, E, and temperature, T_{amb}, can be summarized by using the equation

$$r(E;T) = \rho_E[E - E_{min}(T_{amb})][1 - \rho_T(T - 300)], \quad (1)$$

where $E_{min}(T_{amb})$ is the minimum impact energy needed for the phase transformation to occur, ρ_E is the phase transformation rate per unit impact energy, ρ_T is a positive quantity expressing the magnitude of the decrease of the phase transformation rate per unit temperature increase. It is worth noting that, ρ_T being defined as a positive quantity, the factor $[1 - \rho_T(T - 300)]$ in Eq. (1) takes values lower than unity for $T > 300$ K and decreases as T increases, in agreement with the negative slopes observed in Fig. 8b.

The dependence of $E_{min}(T_{amb})$ on the reactor temperature becomes evident in Fig. 10, where it is plotted as a function of T_{amb}. It can be seen that $E_{min}(T_{amb})$ increases as T_{amb} increases. At least to a first approximation, data seem to arrange according to a linear trend, but experimental uncertainties do not really allow drawing any definite conclusion in this regard.

The dependence of the phase transformation rate on the impact energy E can be rationalized on a relatively simple phenomenological basis. The higher E, the higher the probability to destabilize effectively the initial hcp phase by generating lattice defects. In this respect, the effects of the impact energy can be both intensive and extensive. Intensive effects are related to the fact that, being the volume affected by plastic deformation the same, higher impact energies allow generating a higher density of lattice defects. In contrast, extensive effects can be ascribed to the fact that higher impact energies result in the effective deformation of a larger volume of powder during the impact. Once destabilized, the hcp lattice can then transform into the fcc one according to the microscopic mechanisms proposed in the literature.

However, the same argument fails to explain the increase of the threshold impact energy $E_{min}(T_{amb})$ and the decrease of the phase transformation rate $r(E;T_{amb})$ with T_{amb}. In general, the temperature increase should favour the hcp-to-fcc phase transformation given that it occurs spontaneously when Co powders are heated above 700 K. In addition, higher temperatures should also facilitate the deformation of Co powders during the dynamic compaction process caused by individual impacts and this should enhance the lattice disordering processes eventually responsible for the transition from the hcp to the fcc structure.

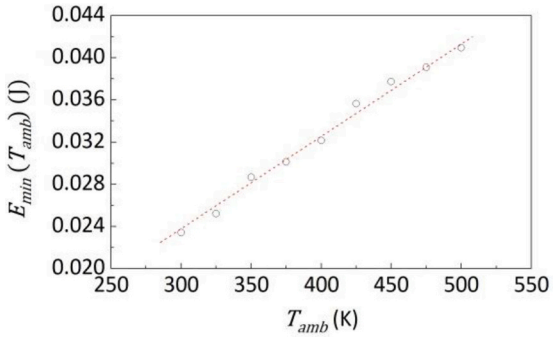

Fig. 10. The minimum impact energy needed for the hcp-to-fcc phase transformation to occur, $E_{min}(T_{amb})$, as a function of the reactor temperature, T_{amb}.

Conversely, the increase of T_{amb} reduces $r(E;T_{amb})$ and determines an increase of $E_{min}(T_{amb})$. This behaviour is quite unexpected, and its understanding requires a deeper analysis of the processes occurring on short time and length scales, involving both experimental and theoretical investigation. This is definitely out of the scope of the present work. However, we can still make an attempt to gain insight into our experimental findings using a simplified model description of mechanically activated phase transformations.

5. Kinetic modelling

We refer to a general kinetic model that relates the global kinetics observed on the macroscopic scale to the statistics underlying the mechanical processing by BM and the local kinetics governing the phase transformation at the length scale of powder particles involved in individual impacts. The model has been described in detail in previous work [59–61]. Here, it is worth reminding that the mechanical processing of powders by BM is inherently discontinuous. The elementary processing event corresponds to the dynamic compaction of the small amounts of powders that get involved during individual impacts. Strain rates are relatively high and the mechanical stresses that spread across the network of contacts between neighbouring particles can locally exceed the yield stress of the processed material. Under such circumstances, effective plastic deformation processes can induce physical and chemical transformations in small volumes v^* irregularly distributed within the total volume of compressed powder. We say that such volumes v^* experience critical loading conditions (CLCs). For the purpose of this work, we assume that the volumes v^* that experience CLCs can undergo the hcp-to-fcc phase transformation.

A second crucial assumption stems straightforwardly from the rheology of Co powders and the effectiveness of their stirring inside the reactor. We noticed that the Co powders we used in our BM experiment remain loose during the mechanical processing regardless of the specific processing conditions. We never observed cold-welding to the reactor bases and side wall or the formation of cohesive compacts. The powders always exhibited remarkable flowability. A consequence of this rheological behaviour is the high degree of mixing that the Co powders can experience during the entire mechanical processing by BM. This is especially true for our BM experiments, which took advantage of the Spex Mixer/Mill 8000 ball mill. Imparting the reactor a three-dimensional swing, this apparatus is particularly effective in stirring loose powders and allow a thorough mixing of powder particles before and after each impact. Therefore, we can assume that the Co powders inside the reactor keep homogeneous during the mechanical processing. It is worth noting that indirect experimental support for this assumption is provided by the reproducibility of the kinetic curves and by their consistent exponential character over the entire range of experimental conditions investigated. Significant deviations from exponential kinetics, or a large scatter in the estimated rate constants, would be expected in the presence of a spatially non-uniform powder distribution. The agreement between experimental data and the kinetic model discussed in the following is consistent with the assumption of powder homogeneity during mechanical processing.

There is another important consequence of the effective stirring of Co powders and the complex three-dimensional motions undergone by the reactor. The ball moves regularly between the two bases and the granular flow accompanies the ball in its displacements. The ball participates in the mixing of powders by directly affecting their flow, increasing the level of disorder in the trajectories of individual powder particles and enhancing the effectiveness of mixing processes [62]. The granular dynamics is so complex that it is impossible to predict which particles will get involved in dynamic compaction processes at impact. Accordingly, we make the simplifying assumption that powder particles are stochastically involved in individual impacts, which means that any given impact affects an amount of powder randomly selected from the whole

powder charge.

The latter assumption implies that volumes v^* are also affected by CLCs stochastically. It follows that the total volume V of powder inside the reactor consists of volumes v^* that have been affected by CLCs different times. We can write that the volume fraction of powder that experiences CLCs during a single impact is

$$k = v/V, \tag{2}$$

where v is the sum of volumes v^* involved in the impact. The relatively low hcp-to-fcc phase transformation rates suggest that κ is much smaller than 1.

According to statistical considerations [59–61], the volume fraction of powder that has undergone CLCs i times after m impacts is

$$\chi_i(m) = \left[(k\,m)^i \Big/ i!\right] \exp(-k\,m), \tag{3}$$

which fulfils the condition

$$\sum_{i=0}^{\infty} \chi_i(m) = 1. \tag{4}$$

Eq. (3) accounts for the statistics underlying the processing of powders by BM. It can be used to relate the phase transformation behaviour at the length scale of volumes v^* to the global kinetics that we observe on the macroscopic scale. To this aim, we associate the progress of the hcp-to-fcc phase transformation in the volume v to the times i it has experienced CLCs. In other words, we write that

$$\chi_{fcc}(m) = \sum_{i=0}^{\infty} \chi_i(m)\chi_{fcc,i}, \tag{5}$$

where $\chi_{fcc,i}$ is the molar fraction of fcc phase in the volume v that has experienced CLCs i times.

We do not have enough information from experiments to reconstruct the functional dependence of $\chi_{fcc,i}$ on i. At present, this is out of reach. However, we remind that the experimental kinetic curve has exponential character. Therefore, also $\chi_{fcc}(m)$ must have exponential character. The simplest way to obtain such exponential character is to assume that [59–61].

$$\chi_{fcc,i} = 1 - \exp(-\kappa\, i) \tag{6}$$

where κ measures the rate constant of the hcp-to-fcc phase transformation at the level of volumes v affected by CLCs.

It is straightforward to show that combining Eqs. (3) and (6) results in the equation [59–61].

$$\chi_{fcc}(m) = 1 - \exp\{-k\,[1 - \exp(-\kappa)]\,m\}, \tag{7}$$

which has exactly the exponential character we were seeking. Indeed,

$$\ln\left[1 - \chi_{fcc}(m)\right] = -k\,[1 - \exp(-\kappa)]\,m. \tag{8}$$

Now, it is worth noting that Eqs. (7) and (8) best fit the experimental kinetic data to a very satisfactory extent. An example is given in Fig. 7.

It appears from Eqs. (7) and (8) that the overall rate constant is equal to $k\,[1 - \exp(-\kappa)]$. It is immediate to see that when κ is relatively large, this expression reduces to k, which means that the entire volume affected by CLCs undergoes the hcp-to-fcc transition. Conversely, when κ is relatively small, the volume involved in the phase transformation is significantly smaller than k.

Of course, the quantity $k\,[1 - \exp(-\kappa)]$ corresponds to $r(E;T)$, which is the rate constant estimated experimentally. Therefore, we must expect that $k\,[1 - \exp(-\kappa)]$ exhibits the same dependence as $r(E;T)$ on impact energy and temperature.

A more systematic assessment of the agreement between model and experimental data can be obtained by considering the full set of kinetic curves collected under all the experimental conditions investigated. The phase transformation rate r was extracted by best-fitting Eq. (7) to each of the 45 kinetic curves corresponding to the five impact energies and nine temperatures explored. The values obtained are reported in Table 2.

It can be seen that r increases with E and decreases with T in a manner consistent with the linear dependences described in the Experimental evidence section. The slope $\partial r/\partial E = \rho_E$, determined by linear regression at constant temperature, takes values in the range 29.1 $\times$ 10^{-5} J^{-1} to 30.8 $\times$ 10^{-5} J^{-1} and remains approximately constant over the entire temperature range investigated, with an average value of 29.7 $\times$ 10^{-5} J^{-1}. Similarly, the slope $\partial r/\partial T = \rho_T$, determined at constant impact energy, varies between -2.6×10^{-3} K^{-1} and -3.2 $\times$ 10^{-3} K^{-1}, with an average of about -2.9×10^{-3} K^{-1} that is independent of the impact energy. The values of ρ_E and ρ_T thus obtained are consistent with those reported in the Experimental evidence section, in agreement with the view that the linear approximations underlying Eqs. (7) and (8) provide a satisfactory description of the kinetics of the hcp-to-fcc phase transformation over the range of conditions explored.

To make progress on this issue, it is necessary to focus on the volume v that experiences CLCs and its possible dependence on impact energy and temperature. First of all, we can imagine that higher E values induce higher local stresses at the level of individual volumes v^*. This could result in larger volumes v^* affected by CLCs and, then, in a faster phase transformation. Additionally, we can suppose that the number of volumes v^* affected by CLCs increases as E increases. Unfortunately, we have no relevant information on the real dependence of v on E. For this reason, we make the simplest possible choice and we assume that v increases linearly with E once the minimum E value needed to induce plastic deformation in Co powders, $E_{min}(T_{amb})$, is exceeded. This implies that k also changes linearly with E.

Concerning the dependence of v on the reactor temperature T_{amb}, we note that the hcp-to-fcc phase transformation of Co powders is caused by the plastic deformation of the hcp lattice and the consequent accumulation of lattice defects [40–49]. However, we know that defective structures typically undergo relaxation and recovery processes that can cause a decrease in the total population of defects [63–68]. The nature and rate of recovery processes depend on defect mobility and, ultimately, on temperature. Higher temperatures facilitate recovery via the recombination or annihilation of lattice defects. As a consequence, we can reasonably expect that higher temperatures can determine a decrease of the lattice defects driving the hcp-to-fcc phase transformation in Co. Along the same line, we can surmise that higher temperatures can also induce a decrease of the volume fraction of fcc phase formed in volumes v^* due to the CLCs experienced.

To a very first approximation, the rate of recovery can be expected to scale with the density of lattice defects [63–68]. Under the assumption that the density of lattice defects scales with the volume v affected by CLCs, we can write that

$$dv = -\phi\, v\, dt, \tag{9}$$

where ϕ is a rate constant with the typical Arrhenius-like dependence on

Table 2
Phase transformation rates r ($\times 10^{-5}$) extracted from exponential fitting of the kinetic curves at all experimental conditions investigated.

T (K)	E=0.046 J	E=0.061 J	E=0.077 J	E=0.095 J	E=0.104 J
300	0.72	1.15	1.57	2.16	2.48
325	0.66	1.07	1.48	2.09	2.39
350	0.60	0.99	1.39	2.00	2.30
375	0.55	0.92	1.30	1.92	2.22
400	0.51	0.85	1.22	1.84	2.14
425	0.46	0.78	1.13	1.75	2.05
450	0.42	0.72	1.06	1.68	1.98
475	0.38	0.65	0.98	1.60	1.89
500	0.34	0.59	0.91	1.52	1.81

temperature that can be expressed as

$$\phi = A\exp(-E_{act}/R\,T). \tag{10}$$

The occurrence of impacts involves that volumes v^* experience a change in temperature due to the local deposition of mechanical energy and the generation of heat. While the local temperature rise is almost instantaneous, the subsequent cooling process takes place on a longer time scale. Cooling can be described by the Newton's law

$$(T - T_{amb})/(T_{max} - T_{amb}) = \exp(-\gamma\, t), \tag{11}$$

where T_{max} is the maximum temperature experienced by the volumes v^*, T_{amb} is the ambient temperature, and γ measures the cooling rate. To a very first approximation, we can suppose that the maximum temperature T_{max} varies linearly with the impact energy E and depends on the ambient temperature T_{amb} according to the equation

$$T_{max} = aE + T_{amb}, \tag{12}$$

where a is the proportionality constant between temperature and impact energy.

It is also reasonable to suppose that recovery occurs at an acceptable rate only when atomic mobility is allowed. For simplicity, we can assume that atoms are mobile as far as the temperature T is higher than a certain value T_{thr} lying between T_{max} and T_{amb}. Taking into account Eq. (11), the time interval within which such condition is fulfilled is equal to

$$\tau = \gamma^{-1}\,\ln(T_{max} - T_{amb})/(T_{thr} - T_{amb}). \tag{13}$$

As expected, Eq. (13) indicates that τ increases with T_{max} and decreases with the cooling rate γ. It can be re-written as

$$\tau = -\gamma^{-1}\ln(1 - T_{amb}/T_{thr}) + \ln(a\,E)/T_{thr}. \tag{14}$$

If we approximate the logarithm with the first term of its Taylor expansion we obtain that

$$\tau \approx \gamma^{-1}T_{amb}/T_{thr} + \ln(a\,E)/T_{thr}, \tag{15}$$

which indicates that τ increases approximately linearly with T_{amb}.

Since T_{max} and T_{thr} cannot be very different in our case, we can also suppose that ϕ undergoes a linear change between T_{max} and T_{thr}. Accordingly, during the time interval τ, the rate constant can be expressed as

$$\phi(t) = \phi(T_{max}) - t[\phi(T_{max}) - \phi(T_{thr})]/\tau\,, \tag{16}$$

where

$$\phi(T_{max}) = A\exp(-E_{act}/R\,T_{max}), \tag{17}$$

and

$$\phi(T_{thr}) = A\exp(-E_{act}/R\,T_{thr}). \tag{18}$$

We can substitute Eqs. (16)–(18) into Eq. (9) and integrate Eq. (9), thus obtaining

$$v = v_{max}\exp\{-\tau[\phi(T_{max}) - \phi(T_{thr})]/2\ \}. \tag{19}$$

Given that T_{max} and T_{thr} are relatively close and τ can be expected to be quite short, we can re-write Eq. (19) as

$$v \approx v_{max}\{1 - \tau[\phi(T_{max}) - \phi(T_{thr})]/2\ \}. \tag{20}$$

Now, it is worth noting that Eq. (20) has exactly the same structure as $k\,[1 - \exp(-\kappa)]$. In particular, we can simply divide Eq. (20) by the total volume of Co powder inside the reactor, V, and obtain the expression of the apparent rate constant of the mechanically induced hcp-to-fcc phase transformation with

$$k = v_{max}/V \tag{21}$$

and

$$\exp(-\kappa) = \tau[\phi(T_{max}) - \phi(T_{thr})]/2. \tag{22}$$

As mentioned before, v_{max} can be expected to increase with the impact energy E, while, based on Eq. (16), $[1 - \exp(-\kappa)]$ can be expected to decrease linearly with the ambient temperature T_{amb}. This is exactly the same dependence on E and T_{amb} displayed by the hcp-to-fcc phase transformation rate $r(E;T)$.

Therefore, the crude assumptions that we have made so far are seemingly sufficient to provide a phenomenological rationalization of the experimental evidence we collected. In particular, it seems reasonable to ascribe the unexpected decrease of the hcp-to-fcc phase transformation rate with the reactor temperature to the occurrence of thermally activated recovery processes that reduce the total volume involved in the phase transformation from an initial maximum value v_{max} to a smaller one.

6. Conclusions

We conducted BM experiments on Co powders with the aim of investigating their response to repeated mechanical deformation. To this aim, we used a ball mill that imparts the reactor three-dimensional harmonic motion. Experimental findings indicate that the mechanical processing induces a transformation of Co from the hcp crystalline phase to the fcc one. The phase transformation occurs gradually and displays exponential kinetics over a wide range of milling frequency and reactor temperature.

The increase of the milling frequency from 14 Hz to 22 Hz determines a corresponding increase of the average impact energy approximately from 0.045 J to 0.110 J. In turn, the increase of the impact energy results in an increase of the phase transformation rate, which was measured from the kinetic curves obtained by quantitative XRD analysis. The increase of the phase transformation rate is approximately linear at all the different reactor temperatures at which BM experiments were performed. Best fitted lines suggest the existence of a minimum impact energy threshold below which the phase transformation does not occur. Control experiments confirmed this circumstance.

While the increase of the phase transformation rate with the impact energy is expected, completely unexpected comes the decrease of the phase transformation rate with the reactor temperature. The fact that the hcp-to-fcc phase transformation takes place spontaneously at temperatures above 700 K seemingly suggests that any temperature increase should favour the phase transformation. In our case, the increase of the reactor temperature was expected to induce an increase of the phase transformation rate. Conversely, we find that increasing the reactor temperature from 300 K to 500 K results in an approximately linear decrease of the phase transformation rate.

With the aim of tentatively explaining the experimental evidence, we adopted a phenomenological approach based on a suitably developed kinetic model. We show that a linear change of the phase transformation rate with impact energy and reactor temperature can be expected under specific assumptions. In particular, we assume that the increase of impact energy eventually determines an increase of the total volume of powder effectively deformed during individual impacts, while the increase of the reactor temperature favours the occurrence of recovery processes that reduce the fraction of fcc phase formed as a consequence of individual impacts.

By no means we claim that our simplifying considerations provide a satisfactory physico-chemical model of the phase transformation kinetics in mechanically processed Co powders. On the contrary, we are aware that the complexity of the system we are investigating prevents any simple explanation of the phase behaviour observed. However, the hypothesis that recovery processes can play a role appears quite reasonable. In addition, it leaves the door open to further investigation of the phase transformation behaviour at higher temperatures, where

thermal effects should definitely favour the transformation from the hcp crystalline structure to the fcc one. This is a point that deserves future investigation.

Author contributions: CRediT

Marta Cappai: Investigation, Methodology, Validation, Writing- Reviewing and Editing; **Maria Carta:** Investigation, Methodology, Validation, Writing- Reviewing and Editing; **Giorgio Pia:** Investigation, Methodology, Validation, Writing- Reviewing and Editing; **Francesco Delogu:** Conceptualization, Data curation, Formal analysis, Investigation, Methodology, Project Administration, Resources, Supervision, Validation, Writing- Original draft preparation, Writing- Reviewing and Editing.

CRediT authorship contribution statement

Marta Cappai: Writing – review & editing, Validation, Methodology, Investigation. **Maria Carta:** Writing – review & editing, Validation, Methodology, Investigation. **Giorgio Pia:** Writing – review & editing, Validation, Methodology, Investigation. **Francesco Delogu:** Writing – review & editing, Writing – original draft, Validation, Supervision, Resources, Project administration, Methodology, Investigation, Formal analysis, Data curation, Conceptualization.

Declaration of competing interest

The authors declare that they have no known competing financial interests or personal relationships that could have appeared to influence the work reported in this paper.

Acknowledgements

We acknowledge financial support under the National Recovery and Resilience Plan (NRRP), Mission 4, Component 2, Investment 1.1, Call for tender No. 104 published on 2.2.2022 by the Italian Ministry of University and Research (MUR), funded by the European Union – NextGenerationEU– Project Title GREEner Nanomaterials for Upconversion in Photocatalytic applications GREEN UP – CUP F53D23004970006 - Grant Assignment Decree No. 1064 adopted on 18/07/2023by the Italian Ministry of Ministry of University and Research (MUR).

We also acknowledge financial support under the National Recovery and Resilience Plan (NRRP), Mission 4, Component 2, Investment 1.1, Call for tender No. 1409 published on 14.9.2022 by the Italian Ministry of University and Research (MUR), funded by the European Union – NextGenerationEU– Project Title DEveloping MEchanochemical Technologies to Render Crop-protection Agrochemicals Greener (DEMETRA) – CUP F53D23008940001- Grant Assignment Decree No. 1384 adopted on 01/09/2023 by the Italian Ministry of Ministry of University and Research (MUR).

We acknowledge financial support from IMPACTIVE (Innovative Mechanochemical Processes to synthesize green ACTIVE pharmaceutical ingredients), the research project funded from the European Union's Horizon Europe 2021-2027 research and innovation programme under grant agreement No. 101057286. Funded by the European Union. Views and opinions expressed are however those of the author(s) only and do not necessarily reflect those of the European Union or HADEA. Neither the European Union nor the granting authority can be held responsible for them.

Data availability

Data will be made available on request.

References

[1] L. Takacs, The historical development of mechanochemistry, Chem. Soc. Rev. 42 (2013) 7649, https://doi.org/10.1039/c2cs35442j.
[2] P.Y. Butyagin, Kinetics and nature of mechanochemical reactions, Russ. Chem. Rev. 40 (1971) 901–915, https://doi.org/10.1070/RC1971v040n11ABEH001982.
[3] D. Tan, F. García, Main group mechanochemistry: from curiosity to established protocols, Chem. Soc. Rev. 48 (2019) 2274–2292, https://doi.org/10.1039/C7CS00813A.
[4] C. Suryanarayana, Mechanical alloying and milling, Prog. Mater. Sci. 46 (2001) 1–184, https://doi.org/10.1016/S0079-6425(99)00010-9.
[5] F. Delogu, G. Gorrasi, A. Sorrentino, Fabrication of polymer nanocomposites via ball milling: present status and future perspectives, Prog. Mater. Sci. 86 (2017) 75–126, https://doi.org/10.1016/j.pmatsci.2017.01.003.
[6] V. Šepelák, A. Düvel, M. Wilkening, K.-D. Becker, P. Heitjans, Mechanochemical reactions and syntheses of oxides, Chem. Soc. Rev. 42 (2013) 7507, https://doi.org/10.1039/c2cs35462d.
[7] C. Suryanarayana, Mechanical alloying: a critical review, Mater. Res. Lett. 10 (2022) 619–647, https://doi.org/10.1080/21663831.2022.2075243.
[8] F. Gomollón-Bel, Ten chemical innovations that will change our world: IUPAC identifies emerging technologies in chemistry with potential to make our planet more sustainable, Chem. Int. 41 (2019) 12–17, https://doi.org/10.1515/ci-2019-0203.
[9] S.L. James, C.J. Adams, C. Bolm, D. Braga, P. Collier, T. Friščić, F. Grepioni, K.D. M. Harris, G. Hyett, W. Jones, A. Krebs, J. Mack, L. Maini, A.G. Orpen, I.P. Parkin, W.C. Shearouse, J.W. Steed, D.C. Waddell, Mechanochemistry: opportunities for new and cleaner synthesis, Chem. Soc. Rev. 41 (2012) 413–447, https://doi.org/10.1039/C1CS15171A.
[10] N.R. Rightmire, T.P. Hanusa, Advances in organometallic synthesis with mechanochemical methods, Dalton Trans. 45 (2016) 2352–2362, https://doi.org/10.1039/c5dt03866a.
[11] J.L. Do, T. Friščić, Mechanochemistry: a force of synthesis, ACS Cent. Sci. 3 (2017) 13–19, https://doi.org/10.1021/acscentsci.6b00277.
[12] O. Galant, G. Cerfeda, A.S. McCalmont, S.L. James, A. Porcheddu, F. Delogu, D. E. Crawford, E. Colacino, S. Spatari, Mechanochemistry can reduce life cycle environmental impacts of manufacturing active pharmaceutical ingredients, ACS Sustain. Chem. Eng. 10 (2022) 1430–1439, https://doi.org/10.1021/acssuschemeng.1c06434.
[13] D.E. Crawford, C.K.G. Miskimmin, A.B. Albadarin, G. Walker, S.L. James, Organic synthesis by twin screw extrusion (TSE): continuous, scalable and solvent-free, Green Chem. 19 (2017) 1507–1518, https://doi.org/10.1039/c6gc03413f.
[14] E. Colacino, V. Isoni, D. Crawford, F. García, Upscaling mechanochemistry: challenges and opportunities for sustainable industry, Trends Chem. 3 (2021) 335–339, https://doi.org/10.1016/j.trechm.2021.02.008.
[15] N. Fantozzi, J.-N. Volle, A. Porcheddu, D. Virieux, F. García, E. Colacino, Green metrics in mechanochemistry, Chem. Soc. Rev. 52 (2023) 6680–6714, https://doi.org/10.1039/D2CS00997H.
[16] G. Mulas, F. Delogu, Kinetic behaviour of mechanically induced structural and chemical transformations, in: High-Energy Ball Milling, Elsevier, 2010, pp. 45–62, https://doi.org/10.1533/9781845699444.1.45.
[17] F. Delogu, L. Takacs, Information on the mechanism of mechanochemical reaction from detailed studies of the reaction kinetics, J. Mater. Sci. 53 (2018) 13331–13342, https://doi.org/10.1007/s10853-018-2090-1.
[18] E. Colacino, M. Carta, G. Pia, A. Porcheddu, P.C. Ricci, F. Delogu, Processing and investigation methods in mechanochemical kinetics, ACS Omega 3 (2018) 9196–9209, https://doi.org/10.1021/acsomega.8b01431.
[19] T.H. Courtney, Modeling of mechanical milling and mechanical alloying, Rev. Part. Mater. 2 (1994) 63–116.
[20] P. Baláž, M. Achimovičová, M. Baláž, P. Billik, Z. Cherkezova-Zheleva, J.M. Criado, F. Delogu, E. Dutková, E. Gaffet, F.J. Gotor, R. Kumar, I. Mitov, T. Rojac, M. Senna, A. Streletskii, K. Wieczorek-Ciurowa, Hallmarks of mechanochemistry: from nanoparticles to technology, Chem. Soc. Rev. 42 (2013) 7571, https://doi.org/10.1039/c3cs35468g.
[21] E. Boldyreva, Mechanochemistry of inorganic and organic systems: what is similar, what is different? Chem. Soc. Rev. 42 (2013) 7719, https://doi.org/10.1039/c3cs60052a.
[22] F.Kh. Urakaev, V.V. Boldyrev, Mechanism and kinetics of mechanochemical processes in comminuting devices: 1. theory, Powder Technol. 107 (2000) 93–107, https://doi.org/10.1016/S0032-5910(99)00175-8.
[23] F. Delogu, A mechanistic study of Ag50Cu50 solid solution formation by mechanical alloying, Acta Mater. 56 (2008) 2344–2352, https://doi.org/10.1016/j.actamat.2008.01.024.
[24] F. Delogu, G. Cocco, Relating single-impact events to macrokinetic features in mechanical alloying processes, J. Mater. Synth. Process. 8 (2000) 271–277, https://doi.org/10.1023/A:1011382008963.
[25] S. Humphry-Baker, S. Garroni, F. Delogu, C.A. Schuh, Melt-driven mechanochemical phase transformations in moderately exothermic powder mixtures, Nat. Mater. 15 (2016) 1280–1286, https://doi.org/10.1038/nmat4732.
[26] F.Kh. Urakaev, V.V. Boldyrev, Mechanism and kinetics of mechanochemical processes in comminuting devices: 2. Applications of the theory. Experiment, Powder Technol. 107 (2000) 197–206, https://doi.org/10.1016/S0032-5910(99)00200-4.
[27] G. Cocco, F. Delogu, L. Schiffini, Toward a quantitative understanding of the mechanical alloying process, J. Mater. Synth. Process. 8 (2000) 167–180, https://doi.org/10.1023/A:1011308025376.

[28] F. Delogu, L. Takacs, Mechanochemistry of Ti–C powder mixtures, Acta Mater. 80 (2014) 435–444, https://doi.org/10.1016/j.actamat.2014.08.036.
[29] L. Vugrin, M. Carta, S. Lukin, E. Meštrović, F. Delogu, I. Halasz, Mechanochemical reaction kinetics scales linearly with impact energy, Faraday Discuss. 241 (2023) 217–229, https://doi.org/10.1039/D2FD00083K.
[30] M. Carta, A.L. Sanna, A. Porcheddu, S. Garroni, F. Delogu, Mechanochemical effects underlying the mechanically activated catalytic hydrogenation of carbon monoxide, Sci. Rep. 13 (2023) 2470, https://doi.org/10.1038/s41598-023-28972-8.
[31] L. Vugrin, M. Carta, F. Delogu, I. Halasz, Extending the Hammett correlation to mechanochemical reactions, Chem. Commun. 59 (2023) 1629–1632, https://doi.org/10.1039/D2CC06487A.
[32] M. Carta, L. Vugrin, G. Miletić, M. Juribašić Kulcsár, P.C. Ricci, I. Halasz, F. Delogu, Mechanochemical reactions from individual impacts to global transformation kinetics, Angew. Chem. Int. Ed. 62 (2023) e202308046, https://doi.org/10.1002/anie.202308046.
[33] R.M. Davis, B. McDermott, C.C. Koch, Mechanical alloying of brittle materials, Metall. Trans. A. 19 (1988) 2867–2874, https://doi.org/10.1007/BF02647712.
[34] T. Klassen, U. Herr, R.S. Averback, Ball milling of systems with positive heat of mixing: effect of temperature in Ag-Cu, Acta Mater. 45 (1997) 2921–2930, https://doi.org/10.1016/S1359-6454(96)00388-6.
[35] Y. Chen, T. Halstead, J.S. Williams, Influence of milling temperature and atmosphere on the synthesis of iron nitrides by ball milling, Mater. Sci. Eng. A 206 (1996) 24–29, https://doi.org/10.1016/0921-5093(95)09977-8.
[36] D. Chen, B. Liu, G. Sun, W. Xu, Y. Zhu, Y. An, L. Zhu, X. Ding, J. Zhang, X. Lu, High-temperature ball milling: an efficient method to fabricate Ti and its alloy powder for additive manufacturing, Adv. Powder Technol. 35 (2024) 104377, https://doi.org/10.1016/j.apt.2024.104377.
[37] S. Chen, Y. Jiang, X. Nong, L. Yu, Evolution of temperature-regulated interfaces and phase transformation in titanium powder during ball milling, JOM 78 (2026) 561–576, https://doi.org/10.1007/s11837-025-07836-8.
[38] A. Baran, T.R. Jensen, M. Polański, High-temperature high-pressure reactive ball milling synthesis of Mg-Ni-based solid-state hydrogen storage materials, J. Energy Storage 103 (2024) 114271, https://doi.org/10.1016/j.est.2024.114271.
[39] M. Carta, M. Cappai, G. Pia, F. Delogu, Intensification of a high-temperature phase transformation by ball milling, Scr. Mater. (2026) 117344, https://doi.org/10.1016/j.scriptamat.2026.117344.
[40] O.S. Edwards, H. Lipson, An X-ray study of the transformation of cobalt, J. Inst. Met. 96 (1943) 177–187.
[41] A.R. Troiano, J.L. Tokich, The transformation of cobalt, Trans. Am. Inst. Min. Metall. Eng. 175 (1948) 728–741.
[42] W. Betteridge, The properties of metallic cobalt, Prog. Mater. Sci. 24 (1980) 51–142, https://doi.org/10.1016/0079-6425(79)90004-5.
[43] Z.Q. Kuang, J.X. Zhang, X.H. Zhang, K.F. Liang, P.C.W. Fung, Latent heat in the thermoelastic martensitic transformation of co, Scr. Mater. 42 (2000) 795–799, https://doi.org/10.1016/S1359-6462(00)00297-9.
[44] M. Knapek, P. Minárik, P. Dobroň, J. Šmilauerová, M.M. Celis, E. Hug, F. Chmelík, The effect of different thermal treatment on the allotropic fcc↔hcp transformation and compression behavior of polycrystalline cobalt, Materials 13 (2020) 5775, https://doi.org/10.3390/ma13245775.
[45] M. Knapek, P. Minárik, A. Greš, P. Dobroň, P. Harcuba, T. Tayari, F. Chmelík, In-situ analysis of the effect of residual fcc phase and special grain boundaries on the deformation dynamics in pure cobalt, Mater. Charact. 215 (2024) 114182, https://doi.org/10.1016/j.matchar.2024.114182.
[46] F. Cardellini, G. Mazzone, Thermal and structural study of the h.c.p.-to-f.c.c. transformation in cobalt, Philos. Mag. A 67 (1993) 1289–1300, https://doi.org/10.1080/01418619308225355.
[47] J. Sort, J. Nogués, S. Suriñach, M.D. Baró, Microstructural aspects of the hcp-fcc allotropic phase transformation induced in cobalt by ball milling, Philos. Mag. 83 (2003) 439–455, https://doi.org/10.1080/0141861021000047159.
[48] F. Delogu, Kinetics of allotropic phase transformation in cobalt powders undergoing mechanical processing, Scr. Mater. 58 (2008) 126–129, https://doi.org/10.1016/j.scriptamat.2007.09.021.
[49] R. Sewak, C.C. Dey, D. Toprek, Temperature induced phase transformation in Co, Sci. Rep. 12 (2022), https://doi.org/10.1038/s41598-022-14302-x.
[50] F. Delogu, G. Mulas, M. Monagheddu, L. Schiffini, G. Cocco, Impact characteristics and mechanical alloying processes by ball milling: experimental evaluation and modelling outcomes, J. Non-Equilb. Proc. 11 (2000) 235–269.
[51] F. Delogu, Solid Phase Reactivity under Mechanical Processing Conditions. Structural Evolution and Transformation Kinetics (Ph.D. Thesis), University of Sassari, 1999.
[52] F. Delogu, L. Schiffini, G. Cocco, The invariant laws of the amorphization processes by mechanical alloying, Philos. Mag. A 81 (2001) 1917–1937, https://doi.org/10.1080/01418610010019107.
[53] C. Caravati, F. Delogu, G. Cocco, M. Rustici, Hyperchaotic qualities of the ball motion in a ball milling device, Chaos 9 (1999) 219–226, https://doi.org/10.1063/1.166393.
[54] G. Manai, F. Delogu, M. Rustici, Onset of chaotic dynamics in a ball mill: attractors merging and crisis induced intermittency, Chaos 12 (2002) 601–609, https://doi.org/10.1063/1.1484016.
[55] A. Polo, M. Carta, F. Delogu, M. Rustici, M.A. Budroni, Controlling nonlinear dynamics of milling bodies in mechanochemical devices driven by pendular forcing, Front. Chem. 10 (2022), https://doi.org/10.3389/fchem.2022.915217.
[56] F. Delogu, A mechanistic study of TiO2 anatase-to-rutile phase transformation under mechanical processing conditions, J. Alloys Compd. 468 (2009) 22–27, https://doi.org/10.1016/j.jallcom.2008.01.035.
[57] E. Napolitano, G. Mulas, S. Enzo, F. Delogu, Kinetics of mechanically induced anatase-to-rutile phase transformations under inelastic impact conditions, Acta Mater. 58 (2010) 3798–3804, https://doi.org/10.1016/j.actamat.2010.03.024.
[58] M. Rustici, G. Mulas, G. Cocco, Detecting chaotic attractors in a ball milling process, Mater. Sci. Forum 225-227 (1996) 243–248, https://doi.org/10.4028/www.scientific.net/MSF.225-227.243.
[59] M. Carta, Mechanochemical Transformations: Bridging the Gap between Global and Local Kinetics (Ph.D. thesis), University of Cagliari, 2024.
[60] M. Carta, E. Colacino, F. Delogu, A. Porcheddu, Kinetics of mechanochemical transformations, Phys. Chem. Chem. Phys. 22 (2020) 14489–14502, https://doi.org/10.1039/D0CP01658F.
[61] M. Carta, F. Delogu, A. Porcheddu, A phenomenological kinetic equation for mechanochemical reactions involving highly deformable molecular solids, Phys. Chem. Chem. Phys. 23 (2021) 14178–14194, https://doi.org/10.1039/D1CP01361K.
[62] G. Manai, F. Delogu, L. Schiffini, G. Cocco, Mechanically induced self-propagating combustions: experimental findings and numerical simulation results, J. Mater. Sci. 39 (2004) 5319–5324, https://doi.org/10.1023/B:JMSC.0000039237.93724.e9.
[63] J.W. Martin, R.D. Doherty, B. Cantor, Stability of Microstructure in Metallic Systems, Cambridge University Press, Cambridge, UK, 1997, https://doi.org/10.1017/CBO9780511623134.
[64] M.B. Bever, On the thermodynamics and kinetics of recovery, in: R. Maddin (Ed.), Creep and Recovery, American Society for Metals, Cleveland, OH, 1957, pp. 14–51.
[65] J.H. Driver, Stability of nanostructured metals and alloys, Scr. Mater. 51 (2004) 819–823, https://doi.org/10.1016/j.scriptamat.2004.05.014.
[66] A. Godfrey, Q. Liu, Stored energy and structure in top-down processed nanostructured metals, Scr. Mater. 60 (2009) 1050–1055, https://doi.org/10.1016/j.scriptamat.2009.02.014.
[67] F.J. Humphreys, M. Hatherly, Recrystallization and Related Annealing Phenomena, 2nd ed., Elsevier, Oxford, UK, 2004 https://doi.org/10.1016/B978-0-08-044164-1.X5000-2.
[68] R.A. Vandermeer, N. Hansen, Recovery kinetics of nanostructured aluminum: model and experiment, Acta Mater. 56 (2008) 5719–5727, https://doi.org/10.1016/j.actamat.2008.07.038.

Marta Cappai received her Ph.D. from the University of Cagliari in 2017 and is currently a Researcher at the University of Cagliari. She teaches Metallic Materials Engineering and Materials Science in engineering programs. Her research in Materials Science focuses on microstructural characterization and quantitative modelling of complex materials, with emphasis on durability and materials behaviour under coupled mechanical and physico-chemical conditions. More recently, her research has also expanded to mechanochemical approaches for the synthesis and functionalization of advanced materials.

Maria Carta received her Ph.D. from the University of Cagliari in 2024 with a thesis entitled Mechanochemical transformations: bridging the gap between global and local kinetics. She is currently a postdoctoral researcher at the University of Cagliari. Her research focuses on the kinetics of mechanically activated transformations in organic and inorganic systems, integrating experimental investigation with analytical and numerical modelling. Her work aims to elucidate how individual mechanical impacts govern solid-state transformations in powders and how processing conditions control reaction kinetics.

Giorgio Pia received a degree in Engineering summa cum laude from the University of Cagliari and a Ph.D. in Materials Engineering from the University of Bologna. His doctoral research focused on the quantitative modelling of porous materials, spanning both traditional and advanced materials, with particular attention to heat and mass transport in complex microstructures. He is Associate Professor of Materials Science and Technology at the University of Cagliari. His research centres on predictive and phenomenological modelling of porous materials, transport processes in heterogeneous systems, nanoporous metals, and mechanochemical approaches for the synthesis of advanced materials. He has authored over ninety peer-reviewed publications.

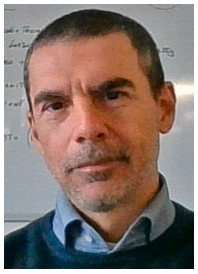

Francesco Delogu received a Master's degree in Chemistry summa cum laude (1995) and a Ph.D. in Chemical Sciences (1999) at the University of Sassari. He is a full professor of Chemical Foundations of Technologies of the University of Cagliari, where he formerly held the positions of assistant professor and associate professor. His research focuses on the kinetics of mechanically activated transformations, the stability of nanocrystalline phases, and the mechanical properties of nanoporous metals. He has authored or co-authored ca. 300 peer-reviewed scientific articles and has participated in several national and international research projects.